buildings

MDPI

Article

Experimental Study on Noise Reduction Performance of Vertical Sound Barrier in Elevated Rail Transit

Lizhong Song [1,2], Yisheng Zhang [1,2], Quanmin Liu [1,2,*], Yunke Luo [3] and Ran Bi [4]

[1] State Key Laboratory of Safety and Resilience of Civil Engineering in Mountain Area, East China Jiaotong University, Nanchang 330013, China; songlizhong@ecjtu.edu.cn (L.S.); 2022138086100050@ecjtu.edu.cn (Y.Z.)
[2] MOE Engineering Research Center of Railway Environmental Vibration and Noise, East China Jiaotong University, Nanchang 330013, China
[3] Department of Civil and Environmental Engineering, The Hong Kong Polytechnic University, Hong Kong 999077, China; yunke.luo@connect.polyu.hk
[4] State Key Laboratory of Bridge Intelligent and Green Construction, Southwest Jiaotong University, Chengdu 611756, China; ran_bi@my.swjtu.edu.cn
* Correspondence: liuquanmin@ecjtu.edu.cn

Abstract: With the large-scale construction of rail transit in mainland China, the noise problem caused by passing trains has become increasingly prominent. The vertical sound barrier is currently the most effective noise control measure for rail transit. However, the noise reduction performance of the vertical sound barrier at different train speeds remains unclear. This study focuses on the box-girder cross-sections of an elevated urban rail transit line with and without vertical sound barriers, conducting field tests during train passages. Based on the test results, the influence of train speed on noise levels at both cross-sections was investigated, the sound source characteristics were analyzed, and the noise reduction performance of the vertical sound barriers at different speeds was explored. The findings indicate the following: Regardless of the presence of sound barriers, within the speed range of 20 to 80 km/h, the linear sound pressure levels at the track-side and beam-side measurement points exhibit a strong linear correlation with speed, while the correlation is weaker at the beam-bottom measurement points. As speed increases, the wheel–rail noise increases by approximately 1.5 dB compared to the structural noise at the same speed. Vertical sound barriers significantly reduce mid-to-high-frequency noise, but in the low frequency band between 20 and 63 Hz, the noise increases, likely due to secondary structural noise radiated by the self-vibration of the barriers when trains pass. At speeds of 20, 40, 60, and 80 km/h, the insertion loss at measurement points located 7.5 m from the track centerline ranges from 6.5 to 9.0, 8.5 to 10.5, 7.5 to 9.5, and 7.5 to 10.2 dB, respectively. At 25 m from the track centerline, the insertion loss ranges from 1.5 to 2.5, 6.0 to 6.5, 5.5 to 6.0, and 5.0 to 6.0 dB, respectively. The noise reduction capability of the vertical sound barrier initially increases and then decreases with higher speeds, and the rate of reduction slows as speed increases. This research will provide a reference and basis for determining speed limits in the rail transit sections equipped with sound barriers.

Keywords: elevated rail transit; different speeds; vertical sound barrier; field test; noise reduction

check for updates

Academic Editor: Humberto Varum

Received: 15 April 2025
Revised: 5 May 2025
Accepted: 9 May 2025
Published: 11 May 2025

Citation: Song, L.; Zhang, Y.; Liu, Q.; Luo, Y.; Bi, R. Experimental Study on Noise Reduction Performance of Vertical Sound Barrier in Elevated Rail Transit. *Buildings* **2025**, *15*, 1621. https://doi.org/10.3390/buildings15101621

Copyright: © 2025 by the authors. Licensee MDPI, Basel, Switzerland. This article is an open access article distributed under the terms and conditions of the Creative Commons Attribution (CC BY) license (https://creativecommons.org/licenses/by/4.0/).

1. Introduction

In recent years, elevated urban rail transit lines have developed rapidly due to their advantages, such as low construction costs and minimal land use. However, the proportion of elevated lines in urban rail transit networks remains relatively low [1]. One of the

significant factors limiting their widespread application is the vibration and noise issues caused by trains passing through elevated sections, which severely affect the lives of residents along the lines [2].

When trains pass over railways, wheel–rail noise is generated due to the interaction between the wheels and rails caused by irregularities in the track [3–7]. Additionally, rail vibrations are transmitted to the bridge structure, leading to bridge-structure noise [8,9]. Furthermore, aerodynamic noise is produced by the friction between the train and the air [10,11], and pantograph–catenary noise arises from the friction between the pantograph and the overhead contact line [12,13]. However, in urban rail transit systems, where operational speeds are generally low (typically not exceeding 120 km/h), the primary sources of noise are wheel–rail noise and bridge-structure noise, with wheel–rail noise being the dominant contributor [14].

Installing sound barriers along the tracks is an effective measure to mitigate the impact of wheel–rail noise on nearby residents. Numerous studies have been conducted by domestic and international scholars on the noise reduction effectiveness of such sound barriers [15–18]. Wang et al. [19] established a numerical prediction model for wheel–rail noise using finite element-boundary element and statistical energy analysis methods, comparing the noise reduction effects of vertical sound barriers and low-height near-rail barriers. Xin et al. [20] analyzed the noise reduction performance of fully enclosed sound barriers on the Jing Xiong Intercity Railway through field tests and numerical simulations, finding a noise reduction of 19.8 to 20.1 dB(A) when trains passed at 350 km/h. Li et al. [21] conducted field tests to study the noise reduction effects of semi-enclosed sound barriers on high-speed railways, showing that the sound insulation of semi-enclosed barriers increases with frequency, providing a noise reduction of 15 to 17 dB(A) within 25 m of the track centerline. Sun et al. [22,23] investigated the noise reduction effects of barriers with different top shapes through surveys and empirical formulas, offering references for sound barrier selection. Jung et al. [24] compared the noise reduction performance of sound barriers with two different top shapes using field tests and scaled model experiments, concluding that cylindrical-top barriers perform better than vertical reflective barriers of the same height. Zhang et al. [25] analyzed the acoustic performance of vertical and semi-enclosed sound barriers through field tests and numerical simulations, demonstrating that semi-enclosed sound barriers provide better noise reduction, outperforming vertical sound barriers by 6 dB(A). Based on field tests, Liu et al. [26] studied the noise reduction effects of sound barriers with different heights and distances, finding that sound pressure levels increase with distance from the barrier at the same height and decrease with proximity to the ground at the same distance. Song et al. [27] used a 3D dynamic model and a 2.5D acoustic model to analyze the noise reduction effects of vertical sound barriers on U-shaped girder bridges, showing significant effectiveness in reducing wheel–rail noise.

However, testing research on the noise reduction performance of vertical sound barriers on elevated urban rail transit sections under different train speeds is rarely reported. Therefore, this study focuses on the box-girder cross-sections of an elevated urban rail transit line with and without vertical sound barriers, conducting field noise tests during train passages. Based on the test results, the noise reduction performance of vertical sound barriers under different train speeds is analyzed.

2. Field Test

2.1. Overview of the Test Section

On an elevated section of a urban rail transit line, sections without sound barriers and sections with vertical sound barriers were selected to conduct field vibration and noise tests caused by train passages. The elevated line uses a six-carriage Type B train with a

maximum operating speed of 80 km/h. Figure 1 shows the cross-section of this test box beam and test photos. The elevated section employs a 30 m span double-track simply supported concrete box girder, the panel width of the box beam bridge is 9.3 m, the floor width is 4.03 m, the beam height is 1.8 m, the thickness of the top plate within the span is 0.25 m, the thickness of the web is about 0.408 m, the thickness of the bottom plate is 0.25 m, the line spacing is 4 m, and the distance between the beam bottom and the ground is about 2.3 m.

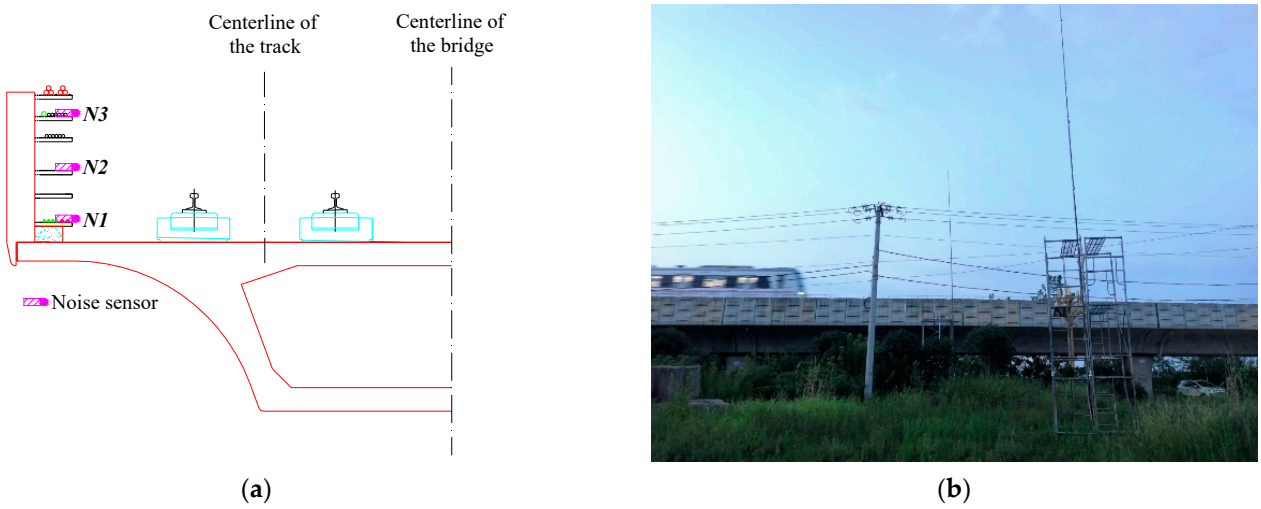


Figure 1. Cross-section of the viaduct box girder section and test photo: (**a**) cross-section of the box girder section; (**b**) photo of the test section.

A 1.6-meter-high retaining wall is installed on both sides of the box girder, with a 2.4-meter-high vertical sound barrier mounted on top of the retaining wall, as shown in Figure 2. The sound barrier primarily consists of H-shaped steel columns, sound-absorbing and insulating panels, and PC transparent sound-insulating panels. The H-shaped steel columns are spaced at intervals of 2.0 m, the sound-absorbing and insulating panels of the barrier are 1.723 m in length and 0.4 m in width, while the PC transparent sound-insulating panels are 1.723 m in length and 1.0 m in width. Both sides of the unit panels are fixed with 2 mm thick soft rubber pads and connected to the H-shaped steel columns via socket joints. The noise barrier is connected to the bridge retaining wall using high-strength bolts.

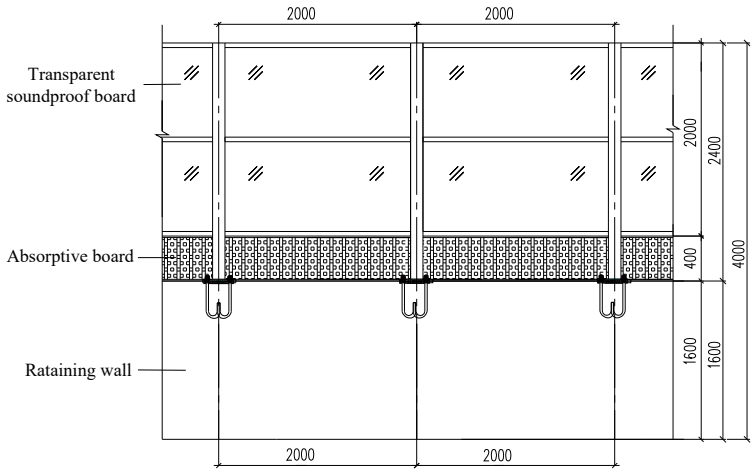


Figure 2. Vertical sound barrier (unit: mm).

2.2. Test Plan

2.2.1. Arrangement of Test Measurement Points

For ease of comparison, noise measurement points were set up at identical locations in both cross-sections to measure the noise caused by trains passing through the elevated urban rail transit section. In strict compliance with ISO 3095: 2013 standards [28], nine noise measurement points were systematically deployed in each of the two cross-sections, with microphones placed beside the outer rail, under the girder, and on the side of the girder to measure the track-side noise, under-girder noise, and side-girder noise, respectively. On the section without a sound barrier, measurement points N1, N2, and N3 are located beside the outer rail, 2.06 m from the track centerline, and at heights of 0.2183 m, 0.7648 m, and 1.3416 m above the bridge deck, (as shown in Figure 3). Measurement points N5 and N6 are located under the girder, 0.3 m from the center of the bottom slab and 1.2 m above the ground, respectively. Measurement points N8, N9, N13, and N14 are located 7.5 m and 25 m from the outer track centerline, at heights of 1.2 m and 3.5 m above the rail surface, respectively. On the section with the vertical sound barrier, the measurement points N1′–N3′, N5′–N6′, N8′–N9′, and N13′–N14′ correspond exactly to the locations of points N1–N3, N5–N6, N8–N9, and N13–N14 on the section without the sound barrier.

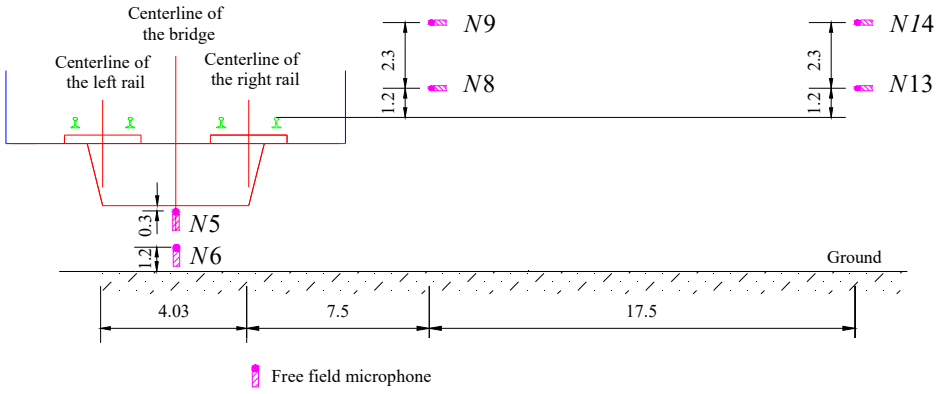


Figure 3. Schematic diagram of test measurement points arrangement.

2.2.2. Test Conditions

The testing was conducted on 2 August 2023 and 9 August 2023. Both tests were conducted at night under similar weather conditions, with a temperature of 25 °C, relative humidity of 81%, no rainfall, windless conditions, etc. Trains passed through the two test sections at speeds of 20 km/h, 40 km/h, 60 km/h, and 80 km/h. To ensure the validity of the test data, five measurements were taken for each speed condition. On the 2nd, 20 sets of valid data were collected for the section without a sound barrier at constant speeds, and on the 9th, 20 sets of valid data were collected for the section with the vertical sound barrier. The measurement points for test data were positioned on the bridge section proximate to the train's travel route.

2.3. Test Equipment

For this test, noise measurements were conducted using GRAS sound sensors. The data acquisition system employed was the DATaRec 4 DIC24 from Head Acoustics, Germany, and ArtemiS data acquisition and analysis software was used for data collection and analysis. This setup is illustrated in Figure 4.



(**a**) (**b**)

Figure 4. Test equipment: (**a**) GRAS sound sensor; (**b**) DATaRec 4 DIC24 data acquisition instrument.

3. Analysis of Test Results

3.1. Impact of Speed on Noise in Both Sections

3.1.1. Impact of Speed on Noise at the Section Without a Sound Barrier

To investigate the influence of train speed on the noise levels at the section without a sound barrier, noise radiation was measured as trains passed through the elevated urban rail transit section at speeds of 20 km/h, 40 km/h, 60 km/h, and 80 km/h. The linear sound pressure level spectra for typical measurement points N1, N5, and N8 under different speed conditions are shown in Figure 5. From Figure 5, the following observations can be made: In general, as the train speed increases, the noise levels at all typical measurement points also increase. Noise levels tend to decrease as the distance from the measurement points to the track increases. In addition, the peak noise frequencies at each measurement point are relatively similar across different speeds. The noise measurement point N1 is located close to the rail and is primarily influenced by wheel–rail noise, with a peak frequency around 800 Hz. A peak appears near 63 Hz in the low-frequency range, which may be attributed to partial background noise interference during the testing process. The noise measurement point N5 is positioned close to the bridge bottom slab and is mainly influenced by bridge-structure noise, with a peak frequency around 63 Hz. The noise measurement point N8 is located on the side of the girder, 7.5 m from the track centerline and 1.2 m above the rail surface, and it is influenced by both wheel–rail noise and bridge-structure noise. The peak frequency in the low-frequency range is around 80 Hz, while in the mid-to-high-frequency range, the peak frequency is around 800 Hz.

To further quantitatively analyze the influence of train speed on the noise levels at the section without a sound barrier, the variation in the linear overall sound pressure level with speed at typical measurement points N1, N5, and N8 is presented. More than five noise tests were conducted under each train speed condition, from which test groups containing background noise (e.g., aircraft noise or dog barking) were removed, retaining five valid test sets, as shown in Figure 6. From Figure 6, the following observations can be made: The linear overall sound pressure levels obtained from the noise tests under the same speed condition at each typical measurement point show little variation, indicating the validity of the noise test data. When the train speed varies between 20 km/h and 80 km/h, the linear overall sound pressure levels at measurement points N1 and N8 exhibit a strong linear correlation with speed. In contrast, the linear overall sound pressure level at measurement point N5, which is more influenced by bridge-structure noise, shows a weaker linear correlation with speed. The noise levels at all typical measurement points increase with higher train speeds. For every 10 km/h increase in speed, the linear overall sound pressure levels at measurement points N1, N5, and N8 increase by approximately 2.3 dB, 1.3 dB, and 1.8 dB, respectively. From the comparison between measurement points

N1 and N5, it can be concluded that, as the train speed increases, wheel–rail noise increases faster than structure noise.

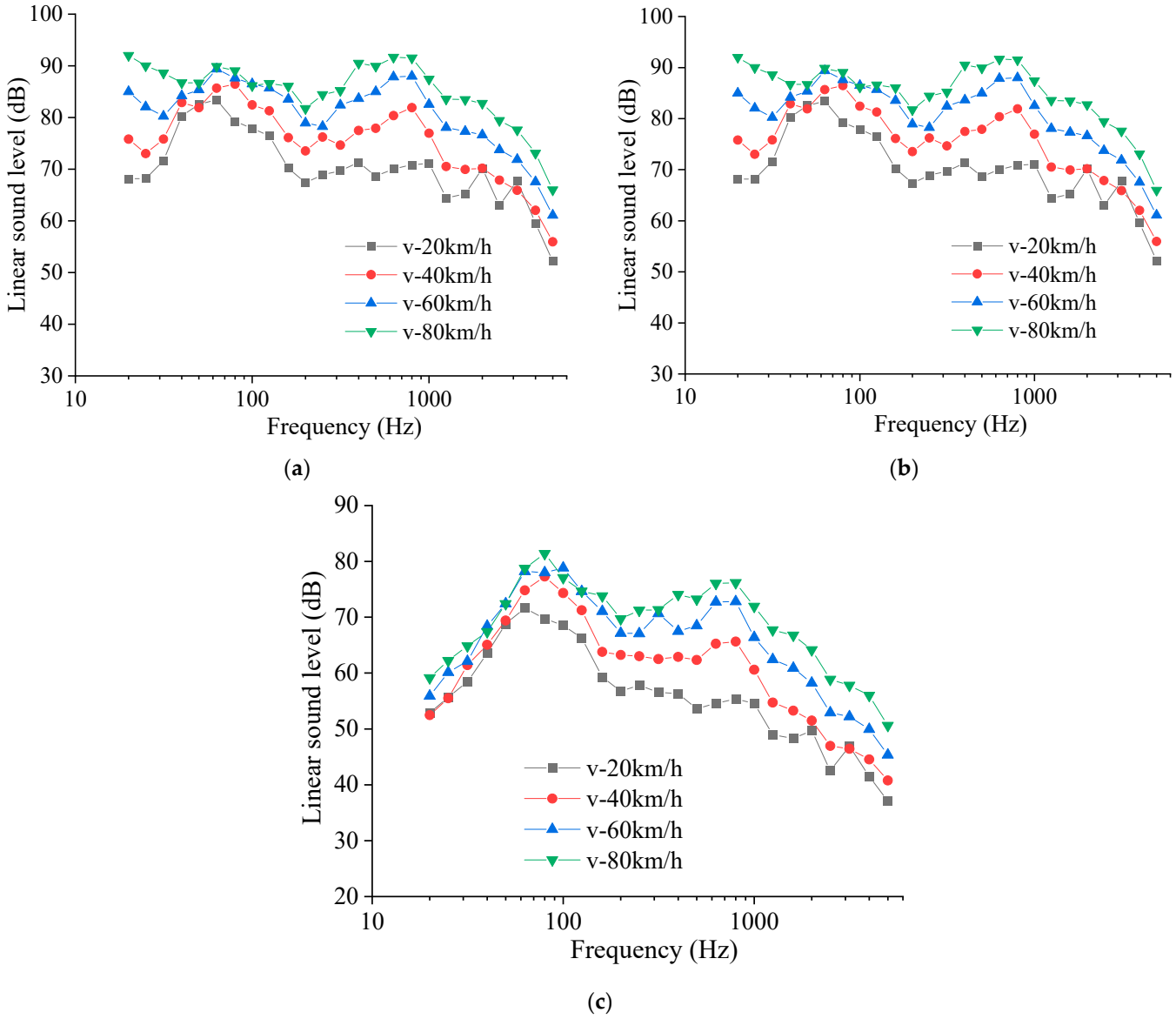


Figure 5. Linear sound-pressure-level spectrum diagram of typical noise measurement points at different speeds/dB: (**a**) measurement point N1; (**b**) measurement point N5; (**c**) measurement point N8.

3.1.2. Impact of Speed on Noise at the Section with a Vertical Sound Barrier

To investigate the influence of train speed on the noise levels at the section with a vertical sound barrier, the noise radiation was measured as trains passed through the elevated urban rail transit section at speeds of 20 km/h, 40 km/h, 60 km/h, and 80 km/h. The linear sound pressure level spectra for typical measurement points N1′, N5′, and N8′ under different speed conditions are shown in Figure 7. From Figure 7, the following observations can be made: In general, as the train speed increases, the noise levels at all typical measurement points also increase. Noise levels tend to decrease as the distance from the measurement points to the track increases. In addition, the peak noise frequencies at each measurement point are relatively similar across different speeds. The noise measurement point N1′ is positioned close to the rail and is mainly influenced by wheel–rail noise, with a peak frequency around 400 Hz in the mid-to-high-frequency range. The noise

measurement point N5′ is positioned close to the bridge deck and is primarily influenced by the structural noise of the bridge, with a peak frequency in the low-frequency range at 80 Hz. The noise measurement point N8′ is situated on the side of the beam and is affected by both wheel–rail noise and bridge-structure noise. It exhibits peaks in both the mid-to-high frequency range and the low-frequency range, with the mid-to-high frequency peak occurring at 800 Hz and the low-frequency peak at 40 Hz.

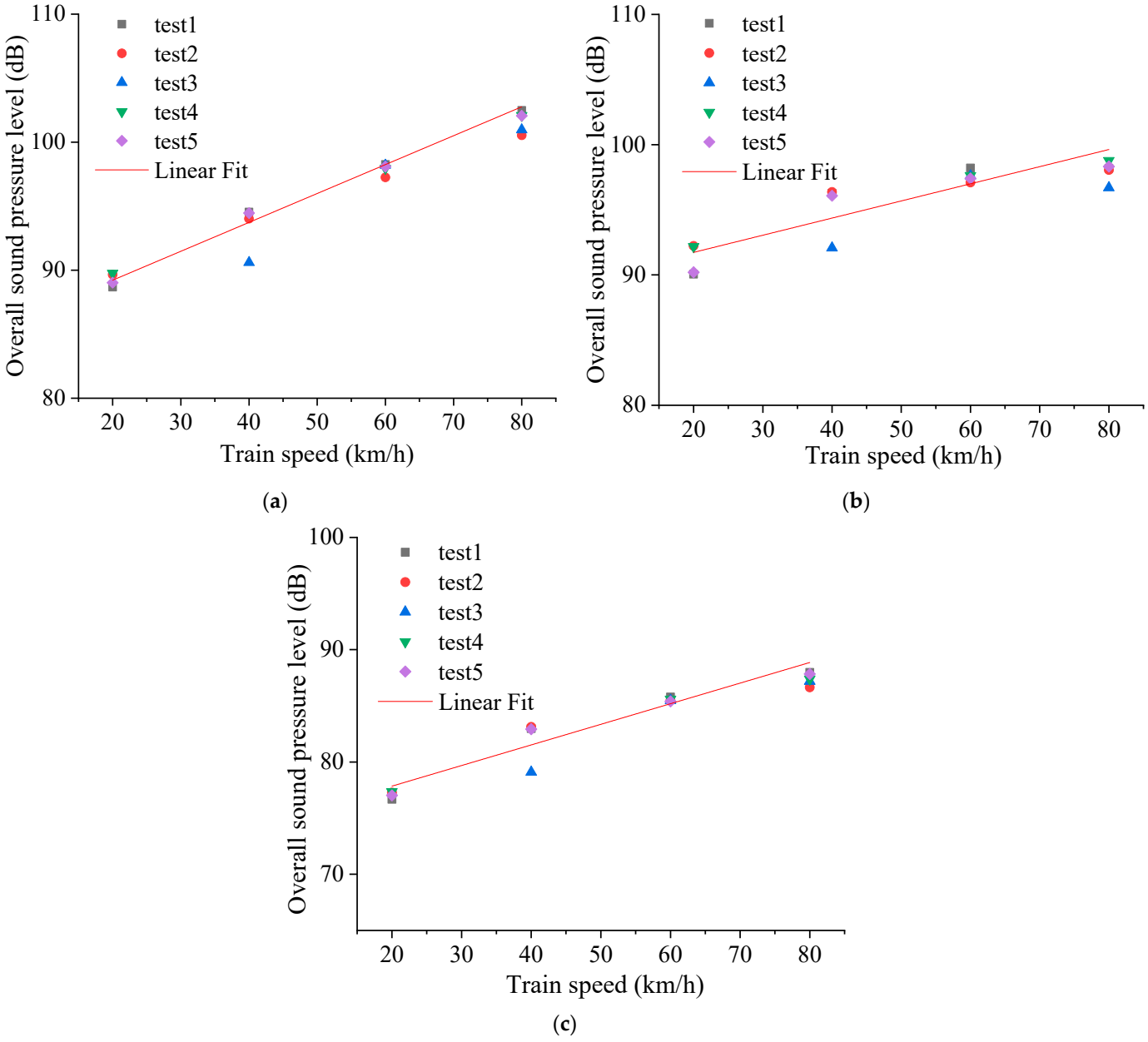


Figure 6. Impact of speed on the linear total sound pressure level of typical noise measurement points: (**a**) measurement point N1; (**b**) measurement point N5; (**c**) measurement point N8.

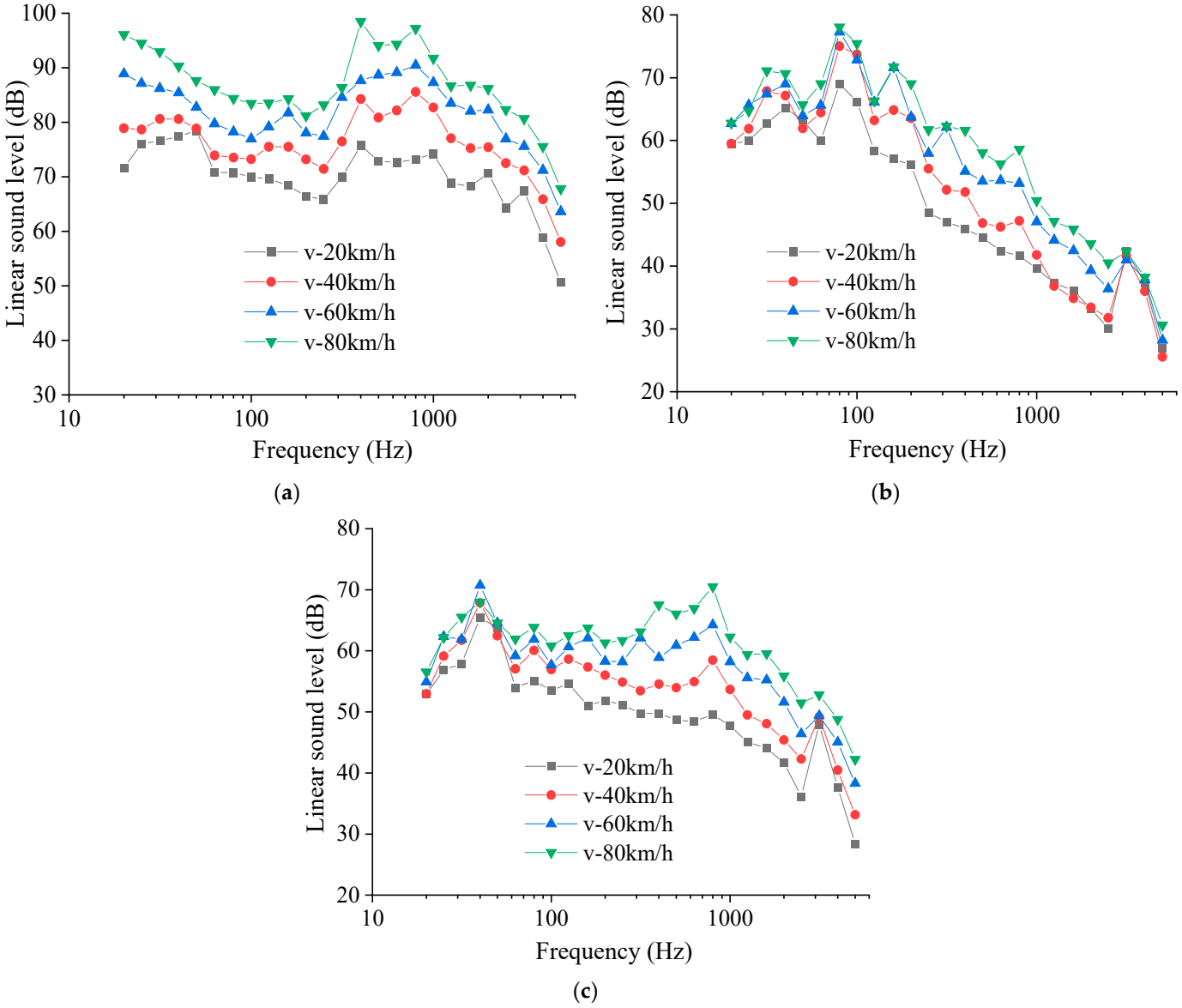


Figure 7. Linear sound-pressure-level spectrum diagram of typical noise measurement points at different speeds/dB: (**a**) measurement point N1′; (**b**) measurement point N5′; (**c**) measurement point N8′.

To further quantitatively analyze the impact of train speed on the noise profile of the vertical sound barrier, the variation in the linear overall sound pressure level with train speed for each typical noise measurement point, N1′, N5′, and N8′ is presented. Noise tests were conducted five times under each speed condition (no aircraft passed by, and dog barking sounds were detected during the test), as shown in Figure 8. From Figure 8, it can be observed that the linear overall sound pressure levels obtained from the noise tests conducted under the same speed condition at each typical measurement point are quite similar, indicating the validity of the noise test data. When the train speed varies from 20 km/h to 80 km/h, there is a strong linear correlation between the linear overall sound pressure level and the train speed for noise measurement points N1′ and N8′, whereas the linear correlation is weaker for measurement point N5′, which is closer to the bottom of the bridge. The noise at each typical measurement point increases with the increase in train speed. For every 10 km/h increase in speed, the linear overall sound pressure levels at measurement points N1′, N5′, and N8′ increase by approximately 3.0 dB, 1.5 dB, and 1.6 dB, respectively. Comparatively, wheel–rail noise increases more rapidly with speed than the structural noise.

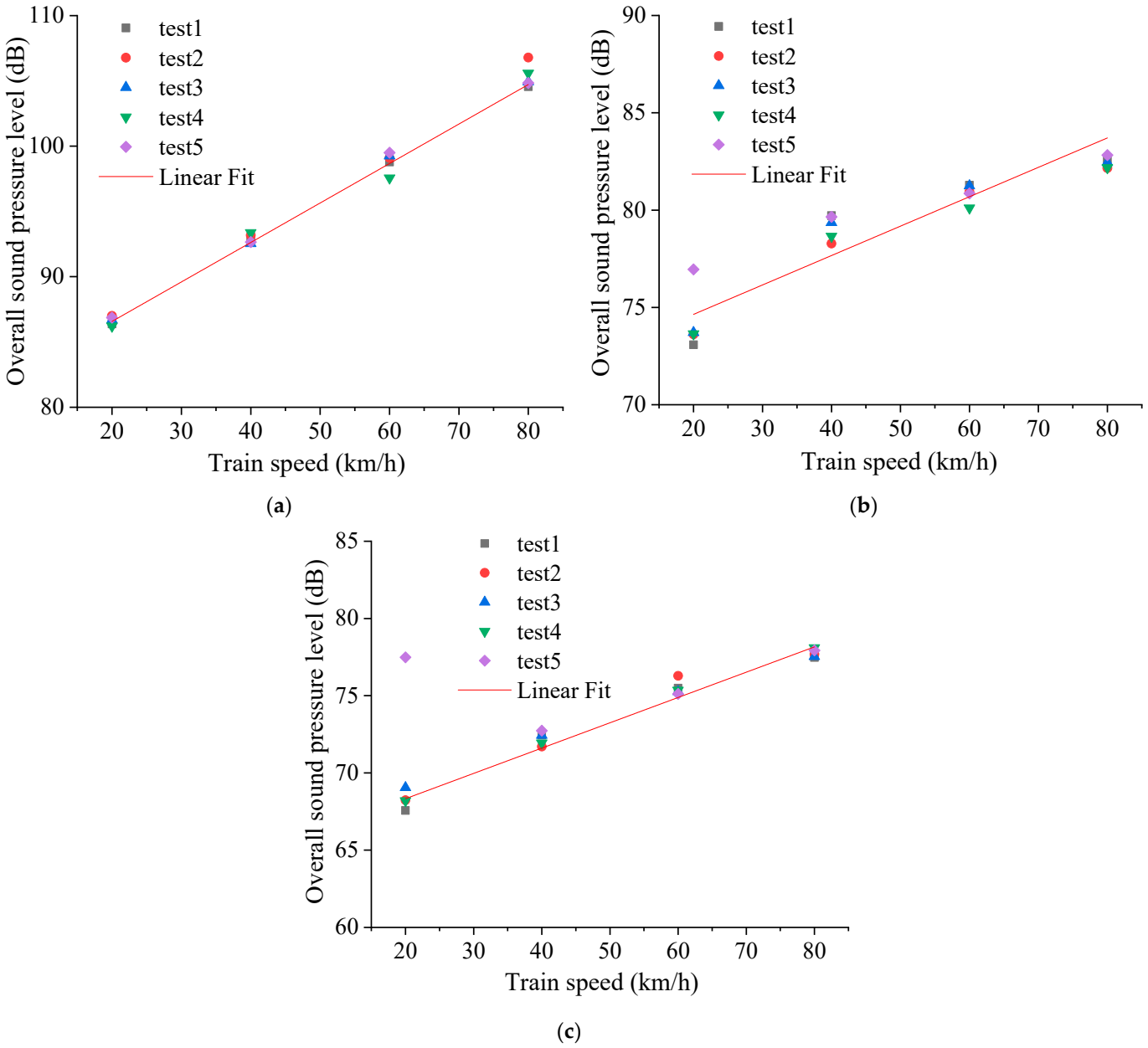


Figure 8. Impact of speed on the linear total sound pressure level of typical noise measurement points: (**a**) measurement point N1′; (**b**) measurement point N5′; (**c**) measurement point N8′.

3.2. Analysis of Sound Source Characteristics in Both Sections

The track-side noise measurement points N1 to N3 and N1′ to N3′ in both sections are located close to the outer rail and are primarily influenced by wheel–rail noise. Meanwhile, the under-beam measurement points N5, N6, N5′, and N6′, situated 0.3 m below the beam and 1.2 m above the ground level, respectively, are mainly affected by the bridge's structural noise. To investigate the amplitude–frequency characteristics of the sound sources in both sections as the train passes through the viaduct, the noise spectrum curves for each typical measurement point at a speed of 80 km/h are provided, along with the total sound pressure level values for these points, as illustrated in Figure 9 and detailed in Table 1.

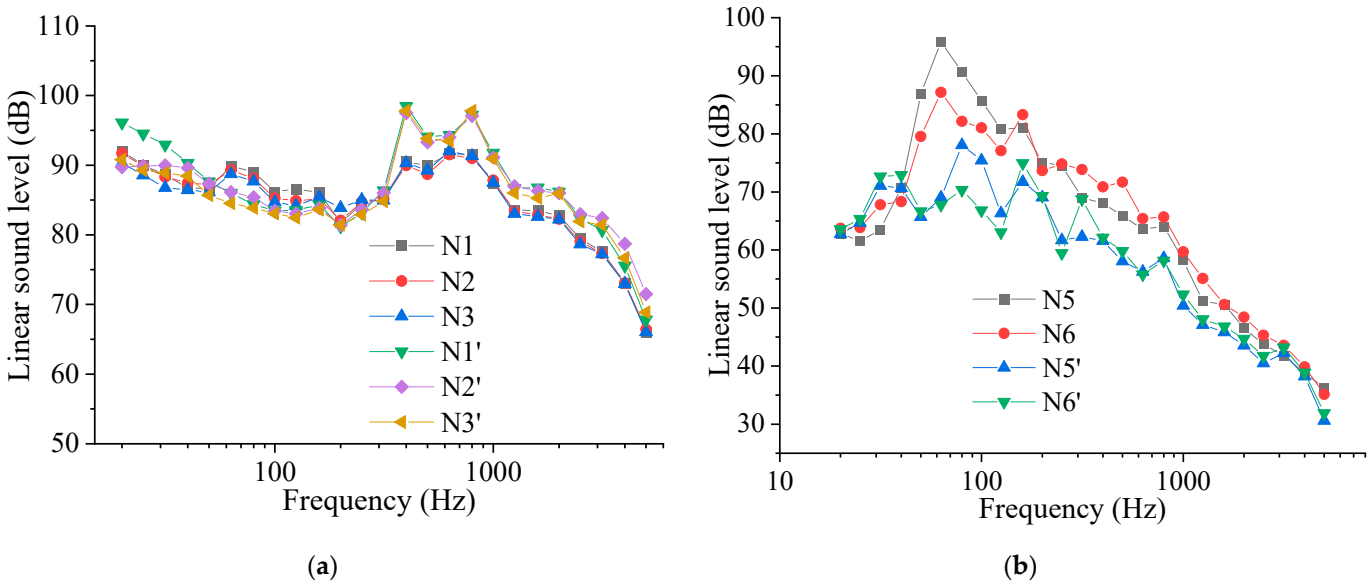


Figure 9. Spectrum curve diagram of track-side and under-beam noise measurement points: (**a**) wheel–rail noise; (**b**) bridge-structure noise.

Table 1. Total sound pressure level of track-side and under-beam noise measurement points (dB).

Section	Measurement Point Number	Total Sound Pressure Level (dB)
Section Without a Sound Barrier	N1	101.58
	N2	101.21
	N3	100.92
	N5	97.97
	N6	91.13
Section with a Vertical Sound Barrier	N1′	105.24
	N2′	103.99
	N3′	104.00
	N5′	82.40
	N6′	80.93

From Figure 9, it can be observed that the linear sound pressure level curves for the noise measurement points N1 to N3 and N1′ to N3′ exhibit some differences in the low-frequency range between 50 and 100 Hz. However, the peak noise frequencies for both sets of points occur between 300 and 1000 Hz, the peak linear sound pressure levels for points N1 to N3 are 91.7 dB, 91.5 dB, and 92 dB, respectively, while for points N1′ to N3′, they are 98.48 dB, 97.49 dB, and 97.82 dB, respectively. This indicates that the linear sound pressure level amplitudes at points N1 to N3 are lower than those at points N1′ to N3′. Similarly, the linear sound pressure level curves for the noise measurement points N5, N6, N5′, and N6′ also show some differences in the low-frequency range between 40 and 200 Hz. The peak noise frequencies for points N5 and N6 occur at 63 Hz, while for points N5′ and N6′, they occur at 80 Hz and 160 Hz, respectively. The peak linear sound pressure levels for points N5 and N6 are 95.90 dB and 87.15 dB, respectively, whereas for points N5′ and N6′, they are 78.06 dB and 74.95 dB, respectively. This suggests that the linear sound pressure level amplitudes at points N5 and N6 are higher than those at points N5′ and N6′.

From Table 1, it can be seen that the total sound pressure levels at the track-side noise measurement points N1 to N3 are 3 to 4 dB lower than those at points N1′ to N3′. In contrast, the total sound pressure levels at the under-beam noise measurement points N5 and N6 are 10 to 16 dB higher than those at points N5′ and N6′.

In summary, there is a difference in the sound source intensity between the two sections, with the section without a sound barrier exhibiting a greater sound source intensity.

3.3. Analysis of Noise Reduction Effect of the Sound Barrier at Different Speeds

From Section 3.2, it is understood that the sound source intensities differ between the section without a sound barrier and the section with a vertical sound barrier; therefore, it is not appropriate to directly compare the sound pressure levels at the corresponding measurement points of the two sections to study the noise reduction effect of the sound barrier at different speeds. To address this, this section first calculates the transmission loss from the track-side noise measurement point N1 (N1′) to the noise measurement points located 7.5 m and 25 m from the centerline of the track at different speeds. Then, by comparing the transmission losses of the two sections, the noise reduction effect of the vertical sound barrier at different speeds is analyzed.

Figures 10 and 11 present the transmission loss spectrum curves for noise measurement points N1-N8, N9, N13, and N14 in the cross-section without a sound barrier, as well as points N1′-N8′, N9′, N13′, and N14′ in the cross-section with a vertical sound barrier, under different train speed conditions. From Figures 10 and 11, it can be observed that the transmission loss spectrum curves for noise measurement points N1 (N1′), in both the cross-section without a sound barrier and the cross-section with a vertical sound barrier, located 7.5 m and 25 m from the track centerline, show similar trends with respect to frequency. As the train speed increases, the peak transmission loss values for both cross-sections also increase. At a speed of 20 km/h, the peak transmission loss frequency for the cross-section without a sound barrier occurs at a high frequency of 3150 Hz. However, at speeds of 40 km/h, 60 km/h, and 80 km/h, the peak transmission loss frequency shifts to a low frequency of 20 Hz. For the cross-section with a vertical sound barrier, the peak transmission loss frequency occurs at high frequencies between 2000 Hz and 2500 Hz at speeds of 20 km/h and 40 km/h. At speeds of 60 km/h and 80 km/h, the peak transmission loss frequency shifts to a low frequency of 20 Hz.

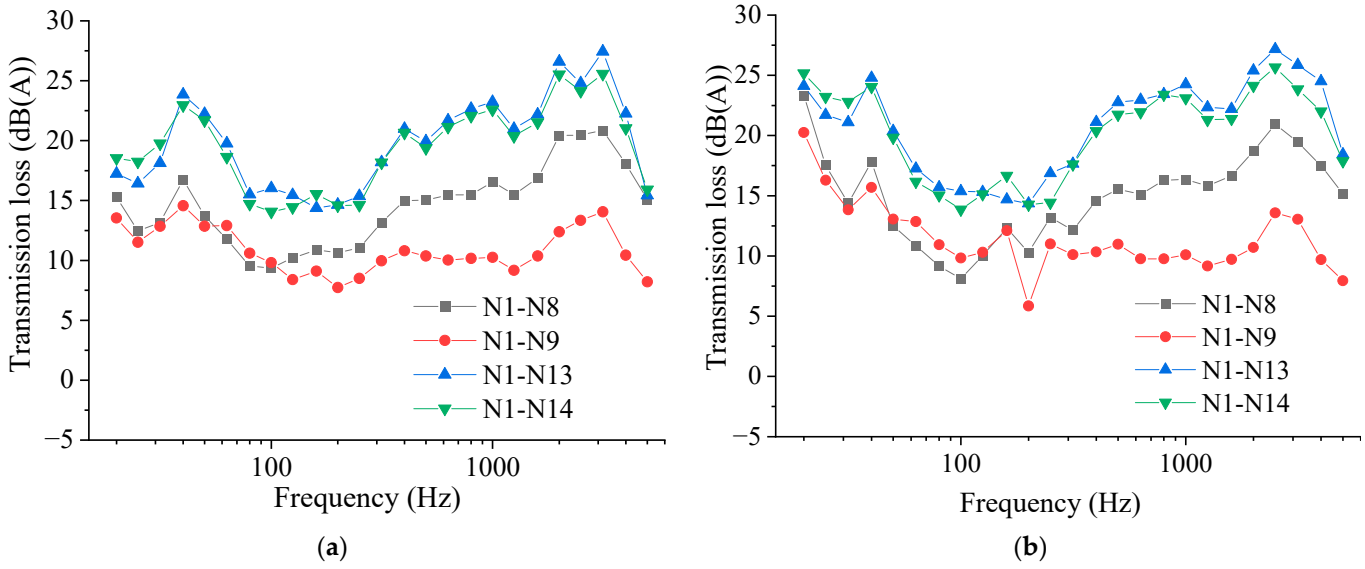


Figure 10. *Cont.*

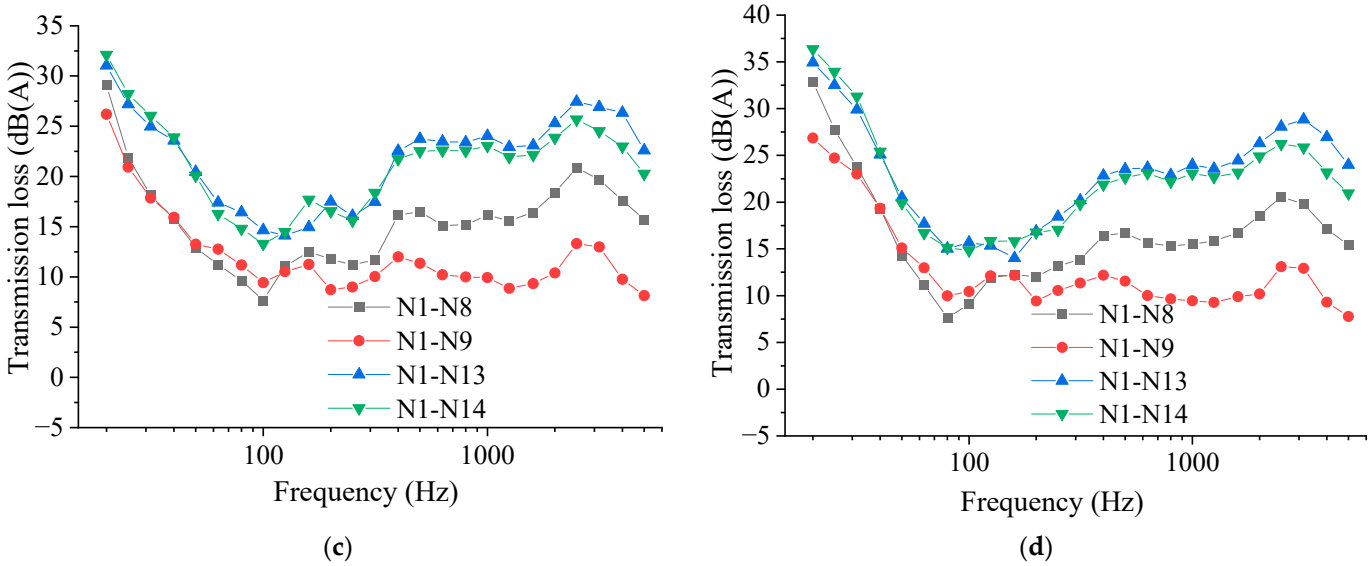


Figure 10. Transmission loss spectrum of the section without a sound barrier: (**a**) 20 km/h; (**b**) 40 km/h; (**c**) 60 km/h; (**d**) 80 km/h.

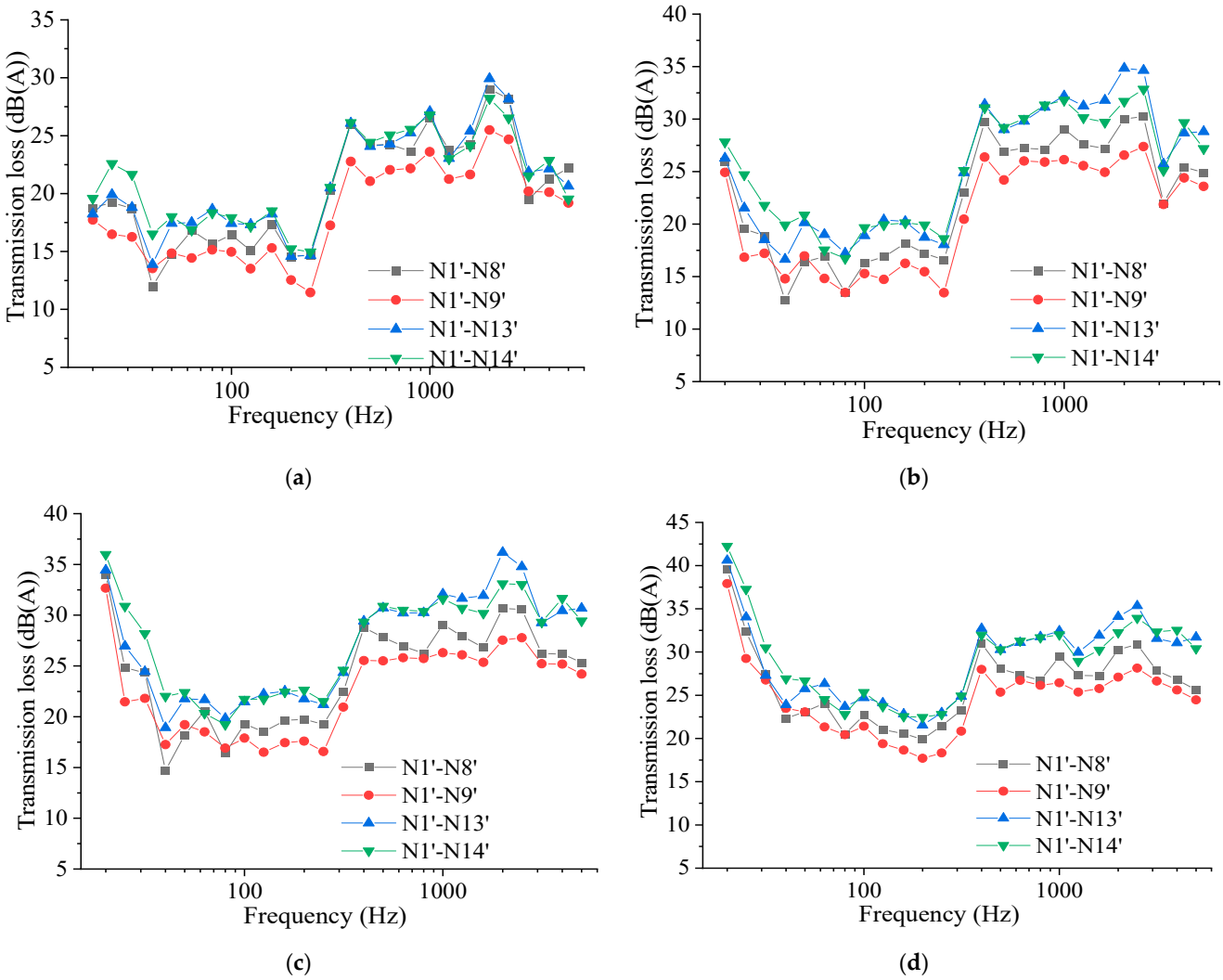


Figure 11. Transmission loss spectrum of the section with a vertical sound barrier: (**a**) 20 km/h; (**b**) 40 km/h; (**c**) 60 km/h; (**d**) 80 km/h.

Figure 12 presents the insertion loss spectra for noise measurement points N8, N9, N13, and N14 under different train speed conditions. From Figure 12, the following observations can be made: The insertion loss spectra curves exhibit similar trends with respect to frequency across different train speeds. The insertion loss initially increases and then decreases as the train speed increases, with the rate of decrease slowing down as the speed increases. In the frequency range of 20~63 Hz, the insertion loss values can be either positive or negative under different speed conditions; however, in the frequency range of 63~5000 Hz, the insertion loss values are predominantly positive, indicating that the vertical sound barrier effectively reduces mid-to-high-frequency noise but may slightly increase noise in the low-frequency range below 63 Hz. This phenomenon is likely due to the vibration of the vertical sound barrier itself, which radiates secondary structural noise when the train passes over the elevated bridge.

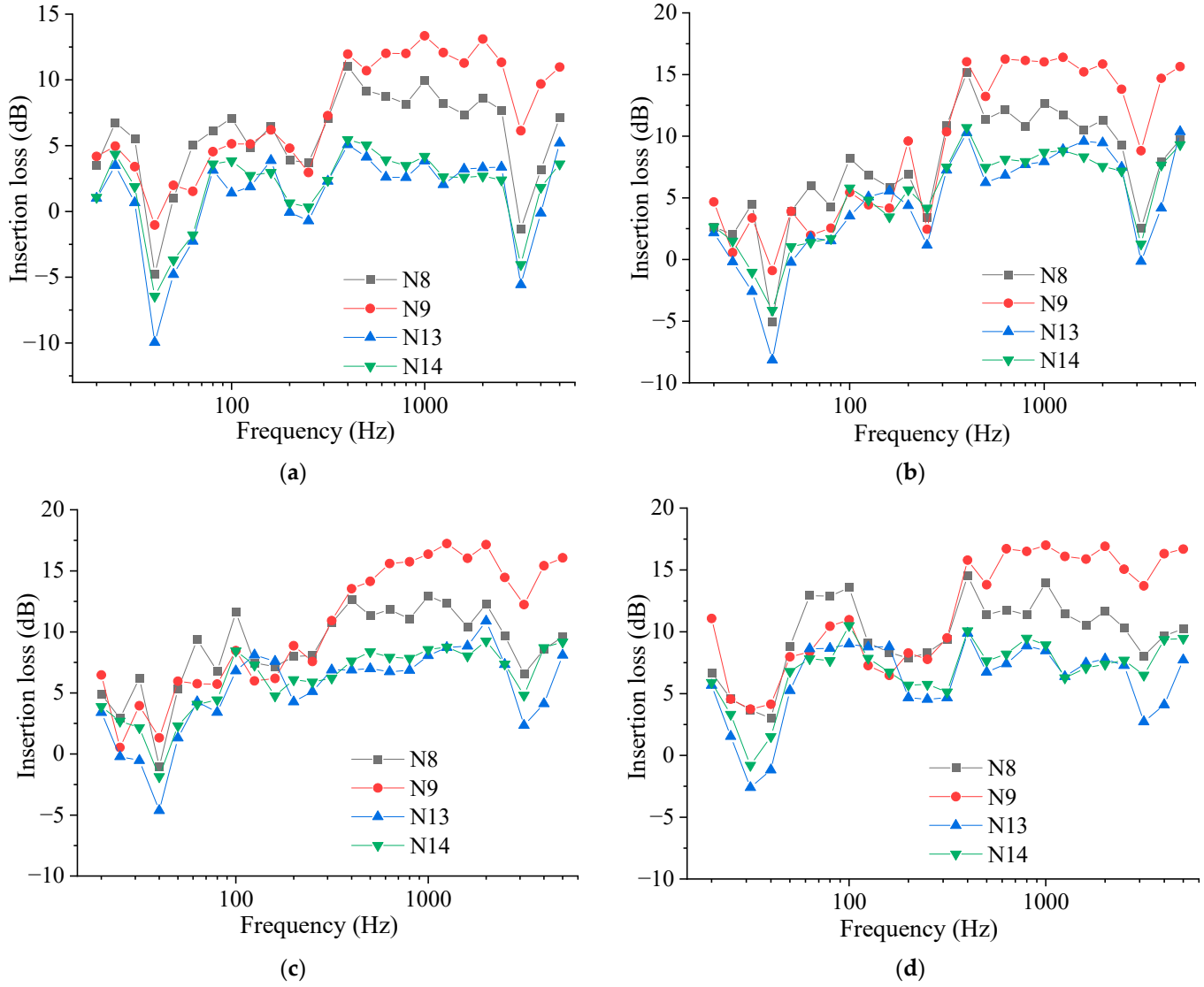


Figure 12. Insertion loss spectrum: (**a**) 20 km/h; (**b**) 40 km/h; (**c**) 60 km/h; (**d**) 80 km/h.

To further quantitatively analyze the noise reduction effect of the vertical sound barrier at different train speeds, Figure 13 presents the insertion loss bar charts for noise measurement points N8, N9, N13, and N14 under different speed conditions. From Figure 13, the following conclusions can be drawn: When the train operates at a speed of 20 km/h, the insertion loss at measurement points located 7.5 m from the outer track centerline ranges from 6.5 to 9.0 dB, while at points 25 m from the outer

track centerline, the insertion loss ranges from 1.5 to 2.5 dB. When the train operates at a speed of 40 km/h, the insertion loss at measurement points located 7.5 m from the outer track centerline ranges from 8.5 to 10.5 dB, while at points 25 m from the outer track centerline, the insertion loss ranges from 6.0 to 6.5 dB. When the train operates at a speed of 60 km/h, the insertion loss at measurement points located 7.5 m from the outer track centerline ranges from 7.5 to 9.5 dB, while at points 25 m from the outer track centerline, the insertion loss ranges from 5.5 to 6.0 dB. When the train operates at a speed of 80 km/h, the insertion loss at measurement points located 7.5 m from the outer track centerline ranges from 7.5 to 10.2 dB, while at points 25 m from the outer track centerline, the insertion loss ranges from 5.0 to 6.0 dB.

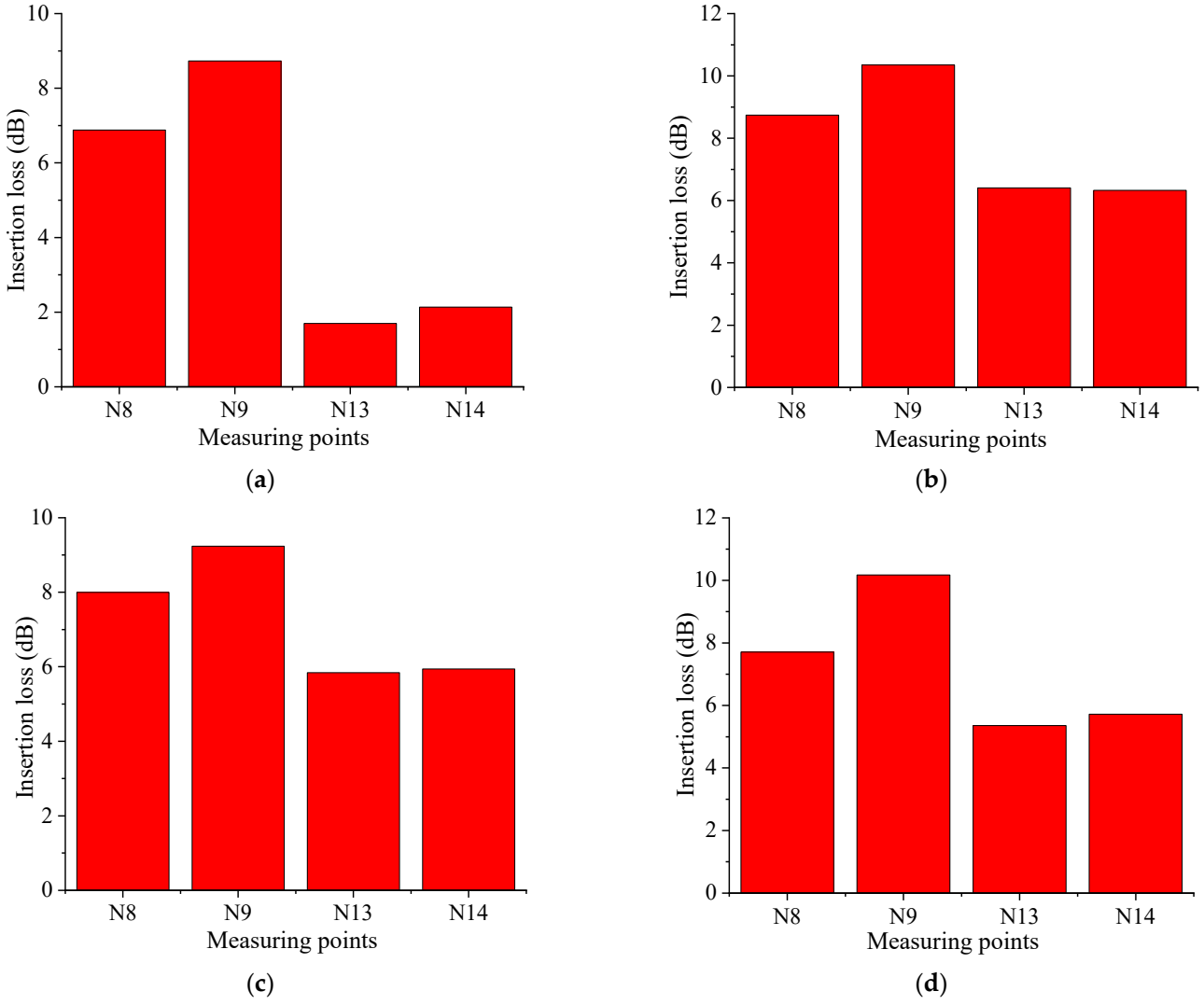


Figure 13. Insertion loss bar chart: (**a**) 20 km/h; (**b**) 40 km/h; (**c**) 60 km/h; (**d**) 80 km/h.

4. Conclusions

This paper focuses on two sections of a viaduct in an urban rail transit system: one without a sound barrier and one with a vertical sound barrier. Through on-site testing, this study evaluates track-side noise, under-beam noise, and beam-side noise for both sections. After data processing and calculations, acoustic characteristics such as the sound-pressure-level spectrum, transmission loss spectrum, insertion loss spectrum, and total sound pressure level at different speed conditions for both sections were obtained. The influence of speed on the noise of both sections was analyzed, and the noise reduction

effect of the vertical sound barrier at different speeds was studied. The main conclusions of this paper are as follows:

(1) Regardless of the presence of a vertical sound barrier, the peak frequency of the linear sound pressure level for the track-side noise measurement point N1 (N1′), which is significantly affected by wheel–rail noise, is in the mid-to-high frequency range. The peak frequency for the under-beam noise measurement point N5 (N5′), which is greatly influenced by bridge structural noise, is in the low-frequency range. The beam-side noise measurement point N8 (N8′), which is affected by both wheel–rail noise and secondary structural noise, has peak frequencies in both the mid-to-high and low-frequency ranges.

(2) When train speed varies between 20 to 80 km/h under both sound barrier and non-barrier configurations, comparatively, the overall sound pressure levels at the track-side and bridge-side measurement points demonstrate stronger linear correlations with train speed than those observed at the under-bridge noise measurement points.

(3) In the section without a sound barrier, for every 10 km/h increase in speed, the linear total sound pressure level at noise measurement points N1, N5, and N8 increases by approximately 2.3 dB, 1.3 dB, and 1.8 dB, respectively. In the section with a vertical sound barrier, for every 10 km/h increase in speed, the linear total sound pressure level at noise measurement points N1′, N5′, and N8′ increases by approximately 3.0 dB, 1.5 dB, and 1.6 dB, respectively.

(4) The vertical sound barrier has an effective noise reduction effect on mid-to-high frequency noise, but there is an increase in noise in the low-frequency range between 20~63 Hz, possibly due to the self-vibration of the sound barrier caused by the train passing over the viaduct, which radiates some secondary structural noise.

(5) At speeds of 20 km/h, 40 km/h, 60 km/h, and 80 km/h, the insertion loss at each noise measurement point located 7.5 m from the outer track centerline ranges from 6.5 to approximately 9.0 dB, 8.5 to 10.5 dB, 7.5 to 9.5 dB, and 7.5 to 10.2 dB, respectively. At 25 m from the outer track centerline, the insertion loss ranges from 1.5 to approximately 2.5 dB, 6.0 to 6.5 dB, 5.5 to 6.0 dB, and 5.0 to 6.0 dB, respectively.

(6) The noise reduction performance of vertical sound barriers exhibits an initial increase, followed by a gradual decrease with rising train speeds, with the rate of decrease diminishing progressively. This phenomenon may be attributed to enhanced low-frequency structure-borne noise radiation induced by wheel–rail contact roughness excitation at elevated speeds, which partially offsets the effectiveness of high-frequency noise attenuation.

This research will provide a reference and basis for setting speed limits in rail transit sections equipped with sound barriers. In the future, theoretical analysis, numerical simulation, and experimental research will be combined to conduct more in-depth studies, so as to provide scientific references and basis for the design and selection of sound barriers.

Author Contributions: Conceptualization, L.S. and Q.L.; methodology, L.S.; software, Y.Z.; formal analysis, Y.Z.; writing—original draft preparation, L.S. and Y.Z.; writing—review and editing, Y.L. and R.B.; project administration, L.S. and Q.L.; funding acquisition, L.S. and Q.L. All authors have read and agreed to the published version of the manuscript.

Funding: This research study was funded by the National Natural Science Foundation of China, grant numbers 52378450 and 52372328; the China Postdoctoral Science Foundation, grant numbers 2023T160214 and 2023M731077; the Natural Science Foundation of Jiangxi Province, grant numbers 20232BAB204087 and 20224BAB214074; and the Postgraduate Innovation Special Fund Project of Jiangxi Province, grant Number YC2023-S541.

Data Availability Statement: The data presented in this study are available upon request from the corresponding author.

Conflicts of Interest: The authors declare no conflicts of interest.

References

1. Hou, X.F.; Feng, C.; Yan, H.M.; Zuo, C. Overview of urban rail transit operations in China's mainland in 2024. *Urban Rapid Rail Transit.* **2025**, *38*, 13–19.
2. Qiu, Y.; Zheng, B.K.; Jiang, B.L.; Jiang, S.; Zou, C. Effect of non-structural components on over-track building vibrations induced by train operations on concrete floor. *Int. J. Struct. Stab. Dyn.* **2025**. [CrossRef]
3. Zhang, X.Y.; Thompson, D.J.; Quaranta, E.; Squicciarini, G. An engineering model for the prediction of the sound radiation from a railway track. *J. Sound Vib.* **2019**, *461*, 114921. [CrossRef]
4. Sheng, X.Z.; Cheng, G.; Thompson, D.J.; Ge, S. Research progress on wheel-rail noise prediction models. *J. Traffic Transp. Eng.* **2021**, *21*, 20–38.
5. Zou, C.; Li, X.; He, C.; Zhou, S.H. An efficient method for estimating building dynamic response due to train operations in tunnel considering transmission path from source to receiver. *Comput. Struct.* **2024**, *305*, 107555. [CrossRef]
6. Li, X.; Zheng, B.; Chen, Y.; Zou, C. A hybrid methodology for estimating train-induced rigid foundation building vibrations. *Constr. Build. Mater.* **2025**, *460*, 139852. [CrossRef]
7. Tao, Z.; Zhang, D.; Tu, D.; He, L.; Zou, C. Prediction of train-induced ground-borne vibration transmission considering parametric uncertainties. *Probabilistic Eng. Mech.* **2025**, *79*, 103731. [CrossRef]
8. Song, X.D.; Wu, D.J.; Li, Q.; Botteldooren, D. Structure-borne low-frequency noise from multi-span bridges: A prediction method and spatial distribution. *J. Sound Vib.* **2016**, *367*, 114–128. [CrossRef]
9. He, Y.P.; Zhang, Y.; Yao, Y.Y.; He, Y.L.; Sheng, X.S. Review on the prediction and control of structural vibration and noise in buildings caused by rail transit. *Buildings* **2023**, *13*, 2310. [CrossRef]
10. Shi, J.W.; Zhang, J.Y.; Li, T. Numerical investigation on aerodynamic noise source identification and far-field noise characteristics of the high-speed train bogie region. *Acoust. Aust.* **2024**, *52*, 375–391. [CrossRef]
11. Wang, B.; Zhang, W.; Wang, F.; Zhao, Q.J.; Cao, C.K.; Gao, Y. Experimental investigation on aerodynamic and noise characteristics of Fenestron. *Chin. J. Aeronaut.* **2023**, *36*, 88–101. [CrossRef]
12. Kang, H.M.; Kim, C.W.; Cho, T.H.; Kim, D.H.; Yoon, S.H.; Kwon, H.B. Investigation for the aerodynamic characteristics of high speed train pantograph with cover. *J. Comput. Fluids Eng.* **2012**, *17*, 18–24. [CrossRef]
13. Li, R.P.; Zhou, N.; Zhang, W.H.; Mei, G.M.; Chen, Z.B. Calculation and analysis of pantograph aerodynamic uplift force. *J. Chin. Railw. Soc.* **2012**, *34*, 26–32.
14. He, J.L.; Wang, Q.; Jiang, W.K. Analysis of the elevated urban rail transit noise. *Urban Rail Transit Res.* **2007**, *10*, 57–60. [CrossRef]
15. Jin, J.Y.; Zhu, C.Y.; Wu, R.; Liu, Y.M.; Li, M. Comparative noise reduction effect of sound barrier based on statistical energy analysis. *J. Comput. Methods Sci. Eng.* **2021**, *21*, 737–745. [CrossRef]
16. Lee, J.; Lee, H.; Kim, I. Reduction effects of shaped noise barrier by composition with adsorbed filter panel. *Int. J. Smart Home* **2016**, *10*, 193–202. [CrossRef]
17. Kim, H.I.; Ahn, S.H.; Park, B.J.; Kim, S.G.; Lee, J.H.; Ko, J.H. The analysis of effect of surface shape and pattern of noise barrier panel on the noise reduction. *J. Korean Soc. Environ. Eng.* **2012**, *34*, 835–839. [CrossRef]
18. Li, Q.T.; Liu, Y.; Luo, Y.Y. Noise reduction prediction of a fully-enclosed sound barrier in urban rail transit systems considering incoherence of sources. *Tongji Daxue Xuebao/Tongji Univ.* **2023**, *51*, 117–125.
19. Wang, C.L.; Zhang, L.T.; Song, L.Z.; Wu, X.L. Predication and analysis of noise reduction of near-rail sound barriers on suburban railways. *J. Noise Vib. Control.* **2022**, *42*, 187–191+278.
20. Xin, S.Y.; Zhang, S.F.; Wang, X.W. Design and research on noise reduction system of fully enclosed sound barrier for beijing-xiong'an intercity railway. *Railw. Stand. Des.* **2022**, *66*, 163–168.
21. Li, X.Z.; Zhao, Q.C.; Zhang, X.; Yang, D.W. Field test and analysis of noise reduction performance of high-speed railway semi-closed sound barriers. *J. Southwest Jiaotong Univ.* **2018**, *53*, 661–669+755.
22. Sun, W.J.; Liu, L.; Yuan, H.L.; Su, Q.P. Influence of top shape on noise reduction effect of high-speed railway noise barrier. *IOP Conf. Ser. Mater. Sci. Eng.* **2019**, *493*, 012043. [CrossRef]
23. Sun, W.J.; Su, Q.P.; Yuan, H.L. Analysis of influencing factors on noise reduction effect of high-speed railway sound barrier. *IOP Conf. Ser. Mater. Sci. Eng.* **2019**, *493*, 012042. [CrossRef]
24. Jung, S.S.; Kim, Y.T.; Cheong, C.U.; Kim, H.C.; Lee, W.S. Noise barrier with top cylindrical tubes. *J. Korean Phys. Soc.* **2006**, *49*, 145–149.
25. Zhang, X.; Liu, R.; Cao, Z.Y.; Wang, X.Y.; Li, X.Z. Acoustic performance of a semi-closed noise barrier installed on a high-speed railway bridge: Measurement and analysis considering actual service conditions. *Measurement* **2019**, *138*, 386–399. [CrossRef]

26. Liu, Y.; Yang, B.; Zhang, P.X.; Zhong, F.Z.; Dong, X.H.; Sun, Y.H. Test and Analysis of Noise Reduction Effect for Different Heights and Distances of Sound Barrier. *J. Adv. Mater. Res.* **2011**, *1269*, 4447–4450. [CrossRef]
27. Song, X.D.; Li, Q. Numerical and experimental study on noise reduction of concrete LRT bridges. *Sci. Total Environ.* **2018**, *643*, 208–224. [CrossRef]
28. *ISO 3095: 2013*; Railway Applications-Acoustics-Measurement of Noise Emitted by Railbound Vehicles. International Organization for Standardization: Geneva, Switzerland, 2013.

Disclaimer/Publisher's Note: The statements, opinions and data contained in all publications are solely those of the individual author(s) and contributor(s) and not of MDPI and/or the editor(s). MDPI and/or the editor(s) disclaim responsibility for any injury to people or property resulting from any ideas, methods, instructions or products referred to in the content.